# UNCERTAINTY MODELING FOR EFFICIENT VISUAL ODOMETRY VIA INERTIAL SENSORS ON MOBILE DEVICES

# SUPPLEMENTARY MATERIAL

# EXPERIMENTAL ANALYSIS OF NOISE ON INERTIAL SENSORS OF ASUS TF201 TABLET DEVICE

*Yağız Aksoy* and A. Aydın Alatan*

Dept. of Electrical and Electronics Engineering, Middle East Technical University, 06800, Ankara

## ABSTRACT

For modeling the uncertainties in a Kalman filter-based system, noise characteristics of the sensors used is very important. This document presents the procedure followed to identify the noise characteristics of the accelerometer and the gyroscope on the utilized device.

## 1. INTRODUCTION

We use the inertial sensor readings to compute the change in pose between consecutive frames. We utilize two inertial sensors: the accelerometer and the gyroscope. The accelerometer readings reflect the sum of the actual acceleration of the device and the gravity vector. We assume an accelerometer that only measures the acceleration of the device and eliminate the gravity vector from the actual accelerometer measurements by using the gravity vector provided by Android system, which utilizes a combination of different sensors to estimate the direction of the gravity. The gyroscope measures the rotational velocity.

Inertial navigation systems generally utilize standalone inertial sensors. Since the main purpose of inertial measurement units on mobile devices is detecting simple gestures, such as orientation change or shake, they are not generally well-suited for odometry applications. It should be noted that characteristics of inertial measurement units on mobile devices are far worse than the ones used in inertial navigation systems. In this section, we analyze the noise characteristics of the sensors on ASUS TF201 Transformer Prime tablet, which is utilized in our experiments.

One of the shortcomings of inertial sensors on mobile devices is low sample rate. For example, the sensors used in [1] deliver readings at 1 kHz, or the ones used in [2] has the sample rate of 1.92 kHz while the mobile device used in [3] records readings at 100 Hz. The device utilized in our system has the sample rate of only 48 Hz.

The other shortcomings, which can be listed as highly varying bias and low signal-to-noise ratio, are analyzed in the following sections.

It should be noted that we utilize the inertial sensors in an augmented reality system for small workspaces. This comes with the characteristic that the translational motion is very small when compared to odometry systems for cars or autonomous robots. As analyzed below, since noise on accelerometers are modeled as an additional Gaussian noise that is independent of the actual acceleration, small actual acceleration results in a lower signal-to-noise ratio (SNR) which makes it harder to extract useful information from the sensors.

Noise characteristics of the accelerometer and the gyroscope of the utilized mobile device are found experimentally. The device is left resting on a still surface for 20 minutes. Since the actual motion is known to be zero, the readings represent the noise on the sensors.

Firstly, the sampling rate of the sensors are found to be 48.53 samples per second. Note that this rate is only slightly higher than the 30 frames per second operation of the camera.

---

*Yağız Aksoy is currently affiliated with Department of Computer Science, ETH Zurich and Disney Research Zurich.
This work was funded by Argela under grant number 4893-01.

## 2. BIAS ANALYSIS

Bias is defined as an additional non-zero term on the noise, which is particularly harmful in the long term operation. As integration of the bias diverges with time, it should be carefully handled in inertial navigation systems.

When bias term is constant on a sensor, it can easily be eliminated by listening to the sensor in resting condition and determining the bias as the mean value of the samples. However, generally, bias changes with sensor turn-on and then varies slowly over time. This requires tracking of bias on the sensors as done in [4, 5]. Tracking of 6 independent biases on 3-axis linear accelerometer and 3-axis gyroscope measurements comes with the price of increased mathematical and computational complexity.

The bias terms on the linear accelerometer and gyroscope are analyzed by taking the average of 1000 consecutive samples. The plots showing the variation of bias terms with time on two sensors can be seen in Figure 1.

Due to the highly varying nature of bias on inertial measurements of the mobile device, it is not an easy task to track them. To prevent the bias terms from causing the inertial navigation from diverging [6], we utilize the inertial measurements only in small time intervals, reducing the effect of the bias terms and hence diminishing the need of determination of instantaneous bias terms on sensor readings.

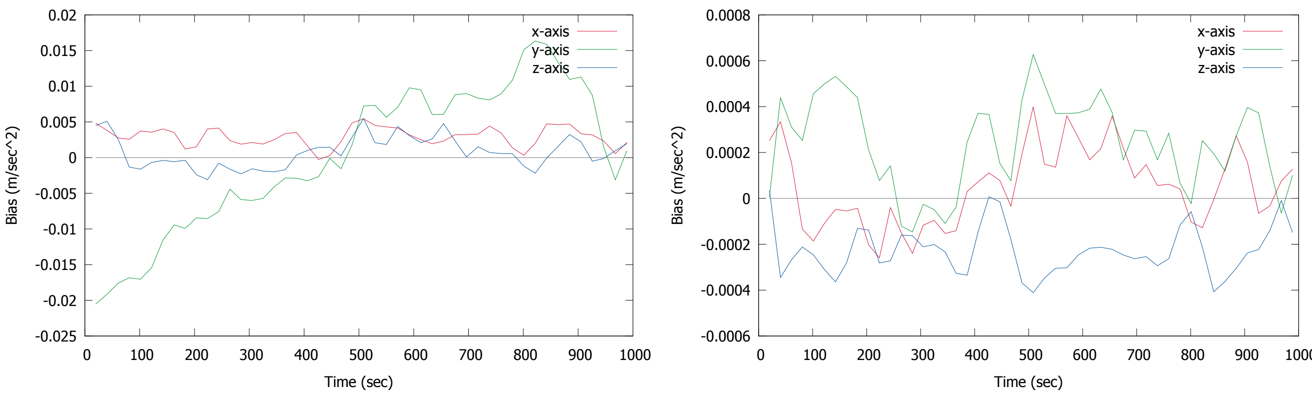


**Fig. 1**: Bias terms on accelerometer and gyroscope readings

## 3. DISTRIBUTION OF NOISE

Figure 3 shows the histogram of sensor readings and their corresponding Gaussian approximations.

Notice that each of the distributions can be effectively approximated by a Gaussian. This is a very important result for the operation for many systems, especially the ones based on a Kalman filter since the filter explicitly requires Gaussian distributed noise on measurements for proper operation.

**Table 1**: Standard deviance of noise on the accelerometer and the gyroscope

| | $x - axis$ | $y - axis$ | $z - axis$ |
|---|---|---|---|
| Accelerometer $(m/s^2)$ | 0.0254 | 0.0311 | 0.0238 |
| Gyroscope $(rad/s)$ | 0.0011 | 0.0008 | 0.0007 |

Variance of the noise on the sensors are presented in Table 1. From these values, covariance matrix $A$ of accelerometer readings $\vec{\alpha}$ and covariance matrix $\Omega$ of gyroscope readings $\vec{\omega}$ can be defined as:

$$A = \begin{bmatrix} 0.0254^2 & 0 & 0 \\ 0 & 0.0311^2 & 0 \\ 0 & 0 & 0.0238^2 \end{bmatrix} \tag{1}$$

$$\Omega = \begin{bmatrix} 0.0011^2 & 0 & 0 \\ 0 & 0.0008^2 & 0 \\ 0 & 0 & 0.0007^2 \end{bmatrix} \tag{2}$$

## 4. POWER SPECTRAL DENSITY ESTIMATION

Power spectral density (PSD) of a signal represents the frequency content of that signal. If $y_n$ denotes a random signal, PSD can be formally defined as:

$$\phi(\omega) = \lim_{N\to\infty} E\left\{ \frac{1}{N} \left| \sum_{n=1}^{N} y_n e^{-i\omega n} \right|^2 \right\} \tag{3}$$

There are several different algorithms for estimating the PSD of a random signal from its samples. The algorithms can be categorized under two main categories: parametric and nonparametric [7]. Parametric approaches need prior knowledge on the shape of the PSD. Nonparametric methods, on the other hand, assumes no underlying structure of the PSD with the price of some decrease in the accuracy.

Since we want to estimate the PSD of the noise signals without a prior knowledge, a nonparametric method known as the *Welch method* [8] is used. This method computes the PSD in overlapping windows of samples of the random sequence and then estimates the actual PSD by taking the average of the computed PSD's of overlapping windows.

The resultant PSD's of the noise on the accelerometer and the gyroscope readings can be seen in Figure 2.

As it can be seen from the PSD's, the noise signal is white except for a DC term, which represents the bias. This is an important result for the operation of the Kalman filter because the filter requires Markov property, which states that the measurements and the inputs to the system should depend only on the previous sample and not the ones before them.

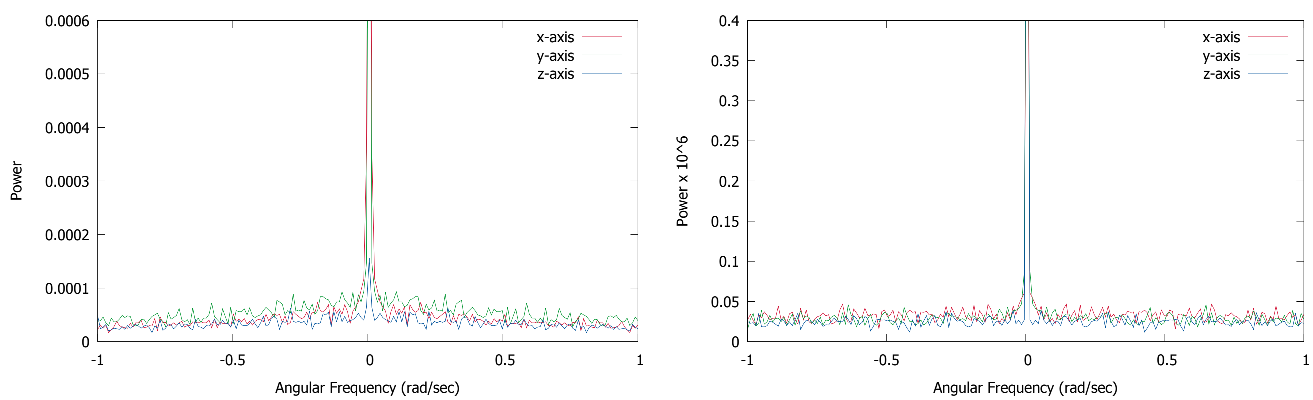


**Fig. 2**: Power spectral density of accelerometer and gyroscope readings

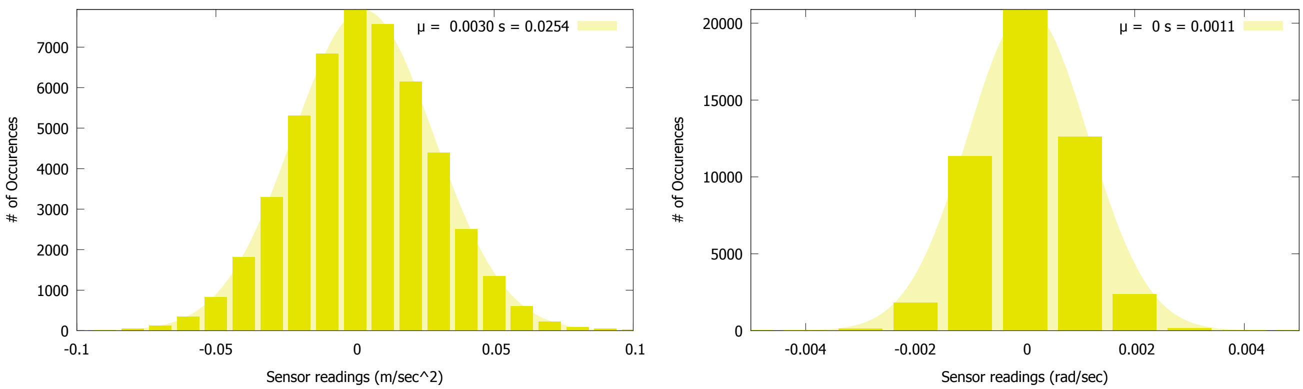


(a) $x - axis$

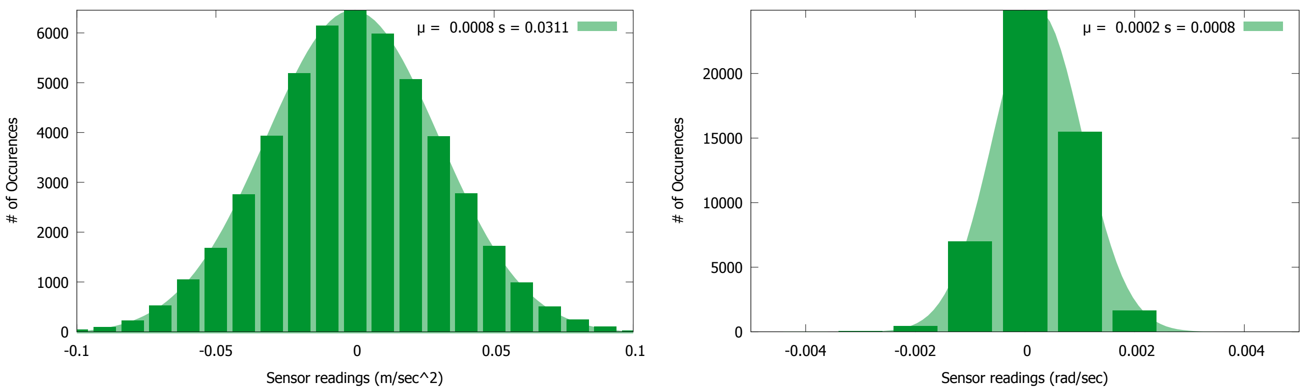


(b) $y - axis$

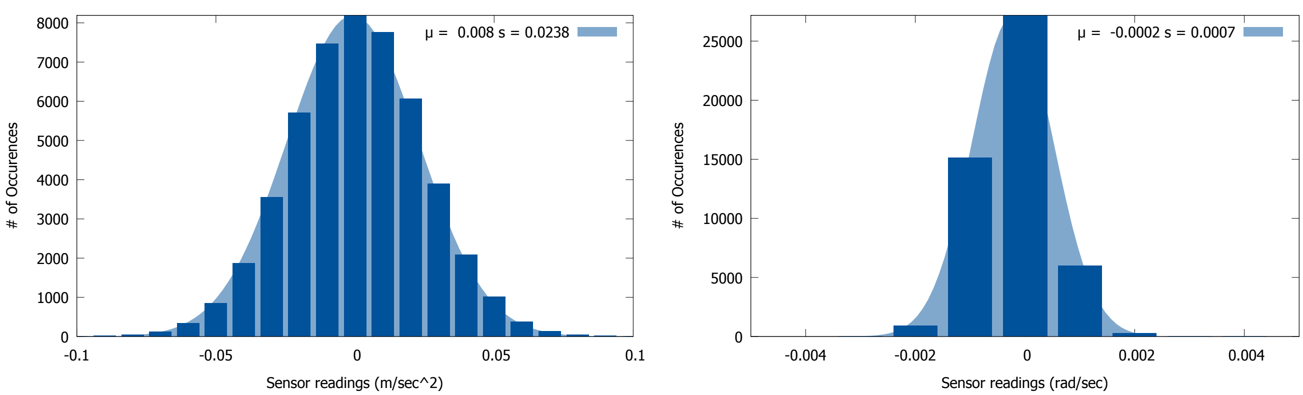


(c) $z - axis$

**Fig. 3**: Distribution of accelerometer and gyroscope readings

## 5. REFERENCES


[1] Suya You and Ulrich Neumann, "Fusion of vision and gyro tracking for robust augmented reality registration," in *IEEE Virtual Reality Conference*, 2001.

[2] Eric Foxlin and Leonid Naimark, "VIS-Tracker: a wearable vision-inertial self-tracker," in *IEEE Virtual Reality Proceedings (VR)*, 2003, pp. 199–206.

[3] Anastasios I. Mourikis and Stergios. I. Roumeliotis, "A multi-state constraint Kalman filter for vision-aided inertial navigation," in *IEEE International Conference on Robotics and Automation (ICRA)*, 2007.

[4] David D. Diel, Paul DeBitetto, and Seth Teller, "Epipolar constraints for vision-aided inertial navigation," in *IEEE Workshop on Motion and Video Computing (WACV/MOTION)*, 2005, vol. 2, pp. 221–228.

[5] Ghazaleh Panahandeh, Dave Zachariah, and Magnus Jansson, "Exploiting ground plane constraints for visual-inertial navigation," in *IEEE/ION Position Location and Navigation Symposium*, 2012.

[6] Bolan Jiang, Ulrich Neumann, and Suya You, "A robust hybrid tracking system for outdoor augmented reality," in *IEEE Virtual Reality Conference (VR)*, 2004, pp. 3–10.

[7] Petre Stoica and Randolph L. Moses, *Introduction to Spectral Analysis*, Prentice Hall, 1997.

[8] Peter D. Welch, "The use of fast fourier transform for the estimation of power spectra: A method based on time averaging over short, modified periodograms," *IEEE Transactions on Audio and Electroacoustics*, vol. 15, no. 2, pp. 70–73, 1967.